Pseudo-Single-Crystalline Self-Assembled Structure Formed from Hydrophilic CdSe and Hydrophobic Au Nanoparticles in the Polystyrene and Poly(4-vinylpyridine) Blocks, Respectively, of a Polystyrene-*b*-poly(4-vinylpyridine) Diblock Copolymer

Ching-Mao Huang and Kung-Hwa Wei*

Department of Materials Science and Engineering, National Chiao Tung University, Hsinchu, Taiwan 30049, ROC

U-Ser Jeng and Hwo-Shuenn Sheu

National Synchrotron Radiation Research Center, 101 Hsin-Ann Road, Science-Based Industrial Park, Hsinchu, Taiwan 30076, ROC

Received June 17, 2008
Revised Manuscript Received August 31, 2008

The composites formed from diblock copolymers and nanoparticles (NPs) have attracted much attention recently because their dimensions are comparable and their applications are versatile;[1] for instance, diblock copolymers can have ordered structures with periodic thicknesses ranging between 10 and 100 nm,[2] while NPs having sizes between 1 and 10 nm have the most interesting optical, electrical, and magnetic properties.[3] Hence, using diblock copolymers as templates to control the spatial locations of NPs is a natural approach to producing hierarchically ordered structures for various applications.[4] In block copolymers, the location of NPs, which critically affects their resulting properties, has been the focus of a number of theoretical and experimental studies.[5−13] For example, using self-consistent field and density functional theories, NPs have been predicted to decorate the interface of two blocks or be positioned in the center of one particular block, depending on the ratio between the size of the NPs and the periodic thickness of the diblock copolymer.[5b] Experimentally, controlling the spatial distributions of NPs in specific domains of block copolymers can be achieved in situ[6] or ex situ,[7] using external fields[8] or directed chemical-binding methods.[9]

The embedding of NPs into a copolymer matrix, however, often occurs with NP-induced morphological transformations in diblock copolymer.[10−13] For instance, simple cubic structures of polystyrene-*b*-poly(ethylene oxide) (PS-*b*-PEO)/CdS NPs composites were obtained when using an originally hexagonally packed cylindrical structure of PS-*b*-PEO.[10a] Similarly, the morphological change of the PS-*b*-P4VP/CdS composite from the hexagonally packed P4VP cylinders into a lamellar structure was induced by the formation of hydrogen bonds between CdS NPs and the P4VP domains.[10b] Moreover, NP-induced phase transformation resulting from the choice of solvent or the depth of the bulk film are also critical factors affecting the particle−concentration gradient along the film depth.[11] Most studies into the ordered morphologies formed from diblock copolymer/NP composites involve only one type of NP; indeed, we are aware of only two reports concerning the formation of ordered structures from two different kinds of NPs and a diblock copolymer: the self-assembly of ex situ-synthesized Au NPs and in situ-synthesized iron oxide NPs on a monolayer film of PS-*b*-P4VP micelles[13a] and the self-assembly of small Au NPs and large Si NPs, both coated with alkyl ligands, along the interface and within the poly(ethylene propylene) core, respectively, of a poly(styrene-*b*-ethylene propylene).[13b] Note, however, that long-range order in the ternary composites consisting of a diblock copolymer and two kinds of NPs has *not* been reported previously.

Herein, we demonstrate, for the first time, that long-range ordered tetragonal single-crystal structures can be formed by loading optimal amounts of hydrophobic Au NPs and hydrophilic CdSe NPs into the respective blocks of a PS-*b*-P4VP. We used high-resolution synchrotron small-angle X-ray scattering (SAXS) and transmission electron microscopy (TEM) to characterize the structures of the PS-*b*-P4VP/CdSe/Au ternary composites.

A lamellar PS-*b*-P4VP diblock copolymer [molecular weight (M_n): 20 000 PS/19 000 P4VP; polydispersity index (M_w/M_n): 1.09; Polymer Source, Inc.] was used in all of the experiments. Hydrophilic pyridine-coated CdSe (CdSe-Py) NPs having a core size of 3.5 nm were synthesized using a modified procedure;[4e] hydrophobic dodecanethiol-coated Au NPs having a core size of 2.5 nm were synthesized using a two-phase method described by Brust et al.[14] Scheme 1 displays the procedures used to fabricate the ternary composites using a two-step process. First, CdSe NPs and PS-*b*-P4VP were dissolved together in pyridine. After evaporation of pyridine, the residue was subject to thermal annealing for a binary PS-*b*-P4VP/CdSe composite. Subsequently, the binary composite and Au NPs were dissolved together in THF. After evaporating THF, the residue was furthermore annealed in dichloromethane for the final product of PS-*b*-P4VP/CdSe/Au ternary composites. Instead of THF,

Scheme 1. Schematic Representation of the Method of Preparation of the PS-*b*-P4VP/CdSe/Au Ternary Composites[a]

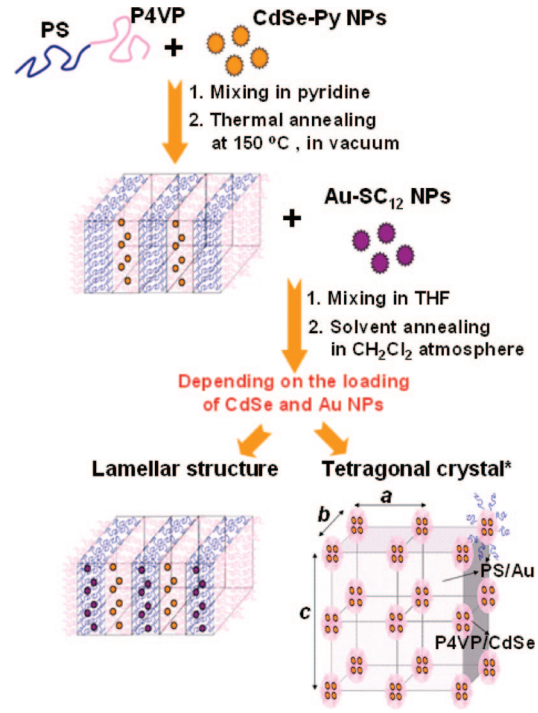

[a] The Au NPs dispersed throughout the continuous PS phase are not presented in the depiction of the tetragonal crystal.

* To whom correspondence should be addressed: Tel +886-35-731871, Fax +886-35-724727, e-mail khwei@mail.nctu.edu.tw.

10.1021/ma801364y CCC: $40.75
Published on Web 09/19/2008

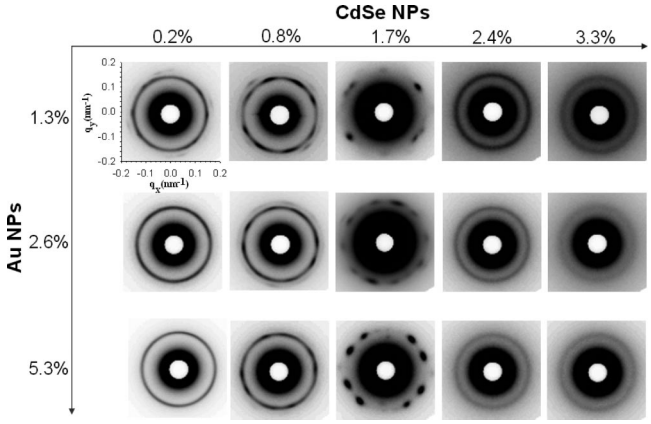

Figure 1. 2D SAXS patterns in the low-Q range ($q = 0.06-0.2$ nm^{-1}) for PS-*b*-P4VP/CdSe/Au ternary composites possessing various NP loadings. The contrast for each pattern is independent.

CH_2Cl_2, of a high evaporation rate at room temperature, was especially used in the solvent annealing process at 30 °C.[11]

The pyridine ligands on the CdSe NPs were removed during the thermal annealing process, allowing the P4VP chains to interact with greater affinity with the CdSe NPs. For this reason, the CdSe NPs were added into the PS-*b*-P4VP prior to adding the Au NPs. When the process was reversed, some of the Au NPs precipitated because the weak interactions between the PS block and the Au NPs could not sequester the Au NPs stably in the PS block when the CdSe NPs were added in pyridine. The volumes of both the Au NP core and the dodecanethiol corona were taken into account in the calculation of the volume fraction of Au NPs in the PS-*b*-P4VP, whereas the volume fraction of the CdSe NPs was calculated on the basis of sizes of the neat CdSe NPs in the absence of surfactant (see Supporting Information for details). TEM analysis was performed using a Hitachi H-600 instrument operated at 100 kV (for higher contrast images). SAXS measurements were performed at the endstation of the BL17B3 beamline of the National Synchrotron Radiation Research Center (NSRRC), Taiwan.[4f]

Figure 1 displays a series of 2-D SAXS images of the nanoparticle/copolymer composites incorporated with various amounts of CdSe and Au NPs. The lamellar rings observed for the composite of a low CdSe NPs concentration of 0.2 vol % indicate that the P4VP/CdSe domains are still dominated by P4VP chains and prefer to phase-separate from the PS phase for the regular lamellar structure of the neat copolymer, regardless the Au NP concentration (1.3−5.3%). As the loadings of nanoparticles increased to 0.3%−0.8% for CdSe NPs and 2.6%−5.3% for Au NPs, reflections other than that of the lamellar structure start to appear, indicating the formation of a new ordered phase; the lamellar structure still contributes to the SAXS patterns. As the CdSe NP concentration reaches 1.7 vol %, the pointlike reflections of the new phase of a single-crystal-like structure replace nearly fully the lamellar powder rings, and the reflection spots are sharpened and intensified upon the increase of the Au NP concentration from 1.3% to 5.3%. As the CdSe NP concentration is up to 2.4 or 3.3 vol %, the isotropic ring patterns present the lamellar structure, regardless of the Au NP concentration. The phenomena can be explained in the following. The actual formation of the final morphology of PS-*b*-P4VP/CdSe/Au composites involves a two-stage process and depends on both the volume fraction of CdSe and Au NPs.

The first stage involves the formation of binary PS-*b*-P4VP/CdSe composites, in which regardless of the CdSe NP concentrations from 0.2 to 3.3 vol %, the PS-*b*-P4VP/CdSe binary composites formed with a lamellar structure after thermal annealing. However, the density of the P4VP−CdSe NP binding increases with the loading of CdSe NPs and the edge-to-edge interparticle distance between CdSe NPs decreases from 14.1 nm at 0.2 vol % CdSe NPs to 3.5 nm at 3.3 vol % CdSe NPs (see the Supporting Information for details). Then, the second stage consists of using THF to dissolve both PS-*b*-P4VP/CdSe composites and dodecanethiol-coated Au NPs and subsequent CH_2Cl_2 solvent annealing. For a low loading with CdSe NPs, such as 0.2 and 0.8 vol %, the degree of P4VP−CdSe binding was not high enough (i.e., P4VP chains are mobile) to prevent P4VP/CdSe lamellae from being dissolved in THF to form a micellar structure that consists of a P4VP/CdSe core and a PS corona. Consequently, the PS-*b*-P4VP/CdSe/Au solution with a low density of P4VP−CdSe NP binding could coalesce into P4VP/CdSe lamellae and PS/Au lamellae during CH_2Cl_2 solvent annealing (Figure S4). As the loading of CdSe NPs increases to 1.7 vol %, the density of P4VP−CdSe NP binding may reach a state that P4VP/CdSe domains have the proper density of P4VP−CdSe binding that is not too high to prevent them from being dissolved in THF. Subsequently, during CH_2Cl_2 solvent annealing process, owing to the presence of dodecanethiol-coated Au NPs in the PS domains, the P4VP/CdSe domains cannot coalesce into lamellar. However, at a higher loading of CdSe NPs, such as 2.4 and 3.3 vol %, the P4VP/CdSe lamellae that experienced thermal annealing, containing a higher density of P4VP−CdSe binding (a high cross-linking density), could not be redissolved in THF completely, so no further phase transition was found in the second stage. In other words, the lamellar morphology of the composites in the first stage has been retained. Consequently, the interesting phase transition from the lamellar structure to the a single-crystal-like structure induced by the CdSe NPs and Au NPs must be crucial, as we cannot find a single-crystal-like structure in the PS-*b*-P4VP/Au or PS-*b*-P4VP/CdSe composite, nor by adding dodecanethiol molecules into the PS-*b*-P4VP/CdSe composite.

Figure 2 displays the SAXS patterns and the corresponding TEM image of the ternary PS-*b*-P4VP/CdSe/Au composite incorporated with 1.7 vol % CdSe NPs and 5.3 vol % Au NPs. Figures 2a,b reveal the single-crystal-like reflections obtained from different sample areas of the ternary composite. Both of the reflections in Figures 2a,b can be grouped into three orientations of the tetragonal cell (Figure 2d), including reflections from the $a \times b$ plane (white indices) and reflections from the twin $a \times c$ (orange indices) and $b \times c$ (red indices) planes at a titled angle of ca. 30° (Figure S5a). Moreover, we have extracted the large cell dimensions to be values of a and b of 48.7 nm and a value of c of 68.9 nm. Lack of diffraction patterns from other orthogonal incident directions, the tetragonal structure cannot be fully confirmed; an alternative support for the tetragonal-like cell, however, is obtained from the TEM image shown below.

Figure 2c displays the corresponding TEM image; the inset presents an enlarged TEM image indicating isolated P4VP/CdSe nanodomains surrounded by a continuous PS/Au phase. The sample volume ($1 \times 1 \times 0.07$ μm^3) under the TEM electron beam was not sufficiently large to produce an electron diffraction pattern comparable to that of SAXS ($500 \times 500 \times 200$ μm^3). A fast Fourier transform (FFT) image (Figure S6a) of the TEM image in Figure 2c revealed two pairs of diffraction patterns with a 4-fold symmetry axis. Furthermore, inverse FFT images (Figure S6) displayed clear 4-fold gridlike patterns. The EDX spectra (Figure S7) confirmed that the CdSe and Au NPs were located in the P4VP nanodomains and PS blocks, respectively.

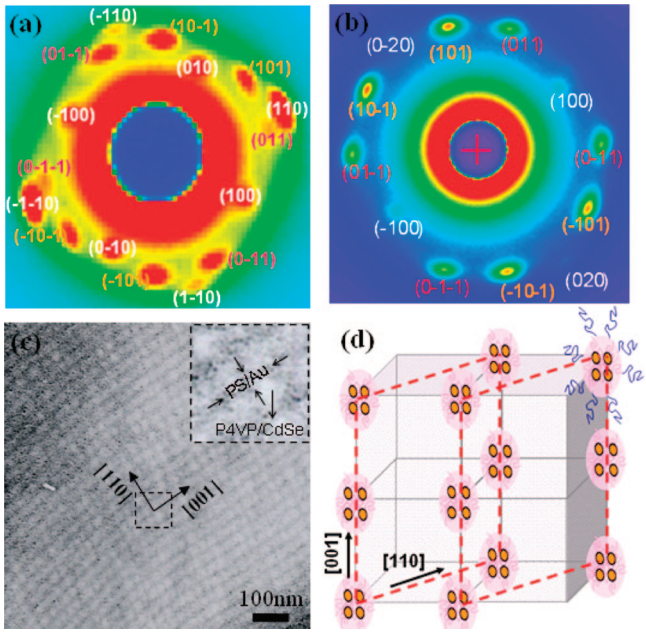

Figure 2. 2D SAXS patterns in low-Q range ($q = 0.06-0.2$ nm^{-1}) for the PS-*b*-P4VP/CdSe/Au composite containing 1.7 vol % CdSe NPs and 5.3 vol % Au NPs. (a, b) The Miller indices are marked according to a tetragonal cell, used to index the diffraction patterns of the *ab* plane (white), superimposed over the tilted *ac* (orange) and *bc* (red) planes. (c) TEM images of PS-*b*-P4VP/1.7 vol % CdSe NPs/5.3 vol % Au NPs ternary composites revealing the [110] and [001] cell directions of the tetragonal cell. The upper-right-hand inset displays an enlarged image. (d) Corresponding orientation for the TEM images.

As a result, we observed a periodic structure for the P4VP/CdSe domains along the in-plane direction of the pristine P4VP lamellae; such in-plane ordering crossed by the neighboring PS/Au layers develops an additional ordering direction perpendicular to the in-plane direction. The two striations visible in the TEM image of the P4VP/CdSe packing (Figure 2c) are the [110] and [001] cell directions of the tetragonal cell, corresponding to the plane (red parallelogram) revealed in Figure 2d, with the characteristic spacing (34 nm) matching well with the *d*-spacing of the (110) (34.4 nm) and (002) (34.4 nm) facets of the tetragonal cell suggested by SAXS.

Figure 3a displays an azimuthal scan of the single-crystal-like pattern in Figure 2b and the relative peaks of each reflection plane. The azimuthal scan also reveals relative sharp reflections having a full width at half-maximum (fwhm) of ca. 2°, which corresponds to the mosaicity of the single-crystal-like structure. Moreover, Figure 3b displays the $I(Q)$ profile taken along a symmetrical scattering direction (10−1) from the image in Figure 2b. We extracted the crystal size to be ca. 0.8 μm using the Debye−Scherrer[16] equation: $D = k\lambda/[\beta \cos(\theta)]$, where D is the thickness of the crystal grain, k is the shape correction constant (normally equal to 0.95 for a spherical particle), λ is the incident X-ray wavelength, β is the fwhm of the Bragg peak, and θ is the Bragg angle. In our case, λ was 1.24 Å and β was 0.0085° (from $Q_{fwhm} = 0.0015$ Å^{-1}).

On the basis of the SAXS and TEM results, we propose a possible route for the formation of the tetragonal cell (Scheme S1). During the first stage, the PS-*b*-P4VP/CdSe composite displays a lamellar structure of a smaller spacing than that of pure PS-*b*-P4VP, with CdSe-free voids at the PS/P4VP interface (corresponding to those in Figure S2a). The formation of these CdSe-free voids in P4VP/CdSe lamellae arose from the PS-*b*-P4VP/CdSe micelles combining to form a roughened PS/P4VP interface during the evaporation of pyridine and the thermal annealing. Subsequently, the PS-*b*-P4VP/CdSe composite and Au NPs were mixed in THF; micelles possessing a P4VP/CdSe core and a PS corona formed, but there should be no interactions between the PS-*b*-P4VP/CdSe micelles and the Au NPs, as evidenced from the related SAXS results (Figure S8). Finally, after removing THF and a subsequent solvent annealing with CH_2Cl_2, the PS-*b*-P4VP/CdSe/Au composite formed a tetragonal-like structure with P4VP/CdSe nanodomains taking the lattice cites in the PS/Au network matrix.

In general, diblock copolymers form body-centered cubic, face-centered cubic, and simple cubic ordered spherical morphologies. In contrast, the ternary PS-*b*-P4VP/CdSe/Au composite incorporating with appropriate CdSe NPs (~1.7 vol %) and Au NPs (1.3−5.3 vol %) can form a tetragonal-like structure, which, for a diblock copolymer, is unusual, especially in diblock copolymer/NP composites; they have been observed previously only under influences of special interactions.[15] Recent studies indicated that modification of interfacial curvature of diblock copolymers through the incorporation of liquid crystalline molecules could also lead to various novel microdomain structures, and a tetragonal packing structure could be obtained with symmetrical PS-*b*-P4VP upon the incorporation with dodecylbenzenesulfonic acid (DBSA).[15b] In our case, a nonspherical distribution of the CdSe nanoparticles (inset of Figure S2) inside the P4VP domains might perturb the originally spherical neat P4VP domains, leading to an anisotropic curvature of the P4VP/CdSe microdomains in the composite, thus, a

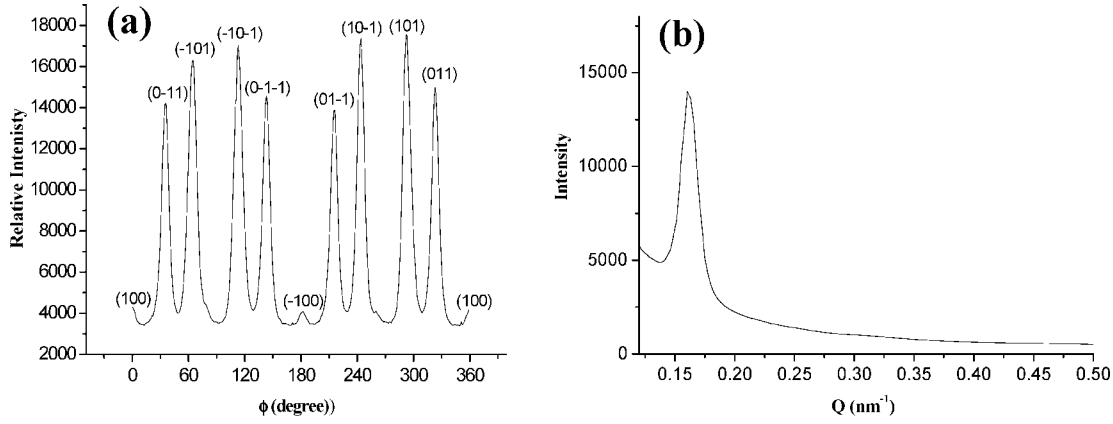

Figure 3. (a) Azimuthal scanning profile of the image in Figure 2b ($Q = 0.161$ nm^{-1}); the (100), (0−1−1), (−101), (−10−1), (0−1−1), (−100), (01−1), (01−1), (10−1), (101), and (011) reflections are found at values of ϕ of 0°, 36°, 65°, 113°, 143°, 180°, 216°, 244°, 293°, and 323°, respectively. (b) SAXS profile obtained along the (101) spot in Figure 2b.

tetragonal micelle packing rather than the conventional BCC packing. The interactions between Au NPs and CdSe NPs might further enhance the anisotropic curvature effect for the long-ranged tetragonal-like structure.

In summary, we have demonstrated that presynthesized hydrophilic CdSe NPs and hydrophobic Au NPs can collectively self-organize in the two distinct blocks of a PS-*b*-P4VP diblock copolymer to form a highly ordered structure. At optimal concentrations of the CdSe NPs and Au NPs, the binding between the P4VP blocks and the CdSe NPs and the weak interactions between the PS blocks and the Au NPs led to dispersion of the two types of NPs in their respective P4VP and PS blocks and subsequent formation of a single-crystalline-like structure comprising P4VP/CdSe nanodomains situated at the apexes of the tetragonal cell and a matrix filled with the PS/Au NP network.

Acknowledgment. We thank the National Science Council, Taiwan, for funding (NSC 95-2120-M-009-007) and the NSRRC, Taiwan, for the SAXS beamtime support. We thank Mr. Yung-Sheng Liu of Chiao Tung University, Miss Kui-Fang Liao of the NSRRC, and Dr. Chiu-Hun Su of the NSRRC for the assistance with the SAXS measurements.

Supporting Information Available: Detailed experimental procedures for the synthesis of the NPs and the preparation of the binary and ternary PS-*b*-P4VP/NP composites; TEM images, SAXS data, and anomalous SAXS profiles of the binary composites; inverse FFT, EDX spectra, and solution-state SAXS data of the ternary composites. This material is available free of charge via the Internet at http://pubs.acs.org.

References and Notes

(1) (a) Förster, S.; Antonietti, M. *Adv. Mater.* **1998**, *10*, 195–217. (b) Bockstaller, M. R.; Mickiewocz, R. A.; Thomas, E. L. *Adv. Mater.* **2005**, *17*, 1331–1349. (c) Haryono, A.; Binder, W. H. *Small* **2006**, *2*, 600–611. (d) Balazs, A. C.; Emrick, T.; Russell, T. P. *Science* **2006**, *314*, 1107–1110.

(2) (a) Chen, J. T.; Thomas, E. L.; Ober, C. K.; Mao, G. P. *Science* **1996**, *273*, 343–346. (b) Morkved, T. L.; Lu, M.; Urbas, A. M.; Ehrichs, E. E.; Jaeger, H. M.; Mansky, P.; Russell, T. P. *Science* **1996**, *52*, 931–933.

(3) Alivisatos, A. P. *Science* **1996**, *271*, 933–937.

(4) (a) Fink, Y.; Urbas, A. M.; Bawendi, M. G.; Joannopoulos, J. D.; Thomas, E. L. *J. Lightwave Technol.* **1999**, *17*, 1963–1969. (b) Lopes, W. A.; Jaeger, H. M. *Nature (London)* **2001**, *414*, 735–738. (c) Naito, K.; Hieda, H.; Sakurai, M.; Kamata, Y.; Asakawa, K. *IEEE Trans. Magn.* **2002**, *38*, 1949–1951. (d) Bockstaller, M. R.; Thomas, E. L. *Phys. Rev. Lett.* **2004**, *93*, 166106. (e) Li, C. P.; Wei, K. H.; Huang, J. Y. *Angew. Chem., Int. Ed.* **2006**, *45*, 1449–1453. (f) Huang, C. M.; Wei, K. H.; Jeng, U. S.; Liang, K. S. *Macromolecules* **2007**, *40*, 5067–5074. (g) Park, S. C.; Kim, B. J.; Hawker, C. J.; Kramer, E. J.; Bang, J.; Ha, J. S. *Macromolecules* **2007**, *40*, 8119–8214.

(5) (a) Huh, J.; Ginzburg, V. V.; Balazs, A. C. *Macromolecules* **2000**, *33*, 8085–8096. (b) Thompson, R. B.; Ginzburg, V. V.; Matsen, M. W.; Balazs, A. C. *Science* **2001**, *292*, 2469–2472. (c) Lee, J. Y.; Thompson, R. B.; Jasnow, D.; Balazs, A. C. *Macromolecules* **2002**, *35*, 4855–4858. (d) Thompson, R. B.; Ginzburg, V. V.; Matsen, M. W.; Balazs, A. C. *Macromolecules* **2002**, *35*, 1060–1071. (e) Lee, J. Y.; Thompson, R. B.; Jasnow, D.; Balazs, A. C. *Phys. Rev. Lett.* **2002**, *89*, 155503. (f) Kim, J. U.; O'Shaughnessy, B. *Phys. Rev. Lett.* **2002**, *89*, 238301. (g) Spontak, R. J.; Shankar, R.; Bowman, M. K.; Krishnan, A. S.; Hamersky, M. W.; Samseth, J.; Bockstaller, M. R.; Rasmussen, K. Ø. *Nano Lett.* **2006**, *6*, 2115–2120. (h) Sides, S. W.; Kim, B. J.; Kramer, E. J.; Fredrickson, G. H. *Phys. Rev. Lett.* **2006**, *96*, 250601.

(6) (a) Spatz, J. P.; Roescher, A.; Sheiko, S.; Krausch, G.; Moller, M. *Adv. Mater.* **1995**, *7*, 731–735. (b) Sohn, B. H.; Seo, B. H.; Seo, B. W.; Yun, S. H.; Park, S. M. *J. Am. Chem. Soc.* **2001**, *123*, 12734–12735.

(7) (a) Hamdoun, B.; Ausserre, D.; Joly, S.; Gallot, Y.; Cabuil, V.; Clinard, C. *J. Phys. IV* **1996**, *6*, 493–501. (b) Weng, C. C.; Wei, K. H. *Chem. Mater.* **2003**, *15*, 2936–2941. (c) Chiu, J. J.; Kim, B. J.; Kramer, E. J.; Pine, D. J. *J. Am. Chem. Soc.* **2005**, *127*, 5036–5037. (d) Lin, Y.; Boker, A.; He, J. B.; Sill, K.; Xiang, H. Q.; Abetz, C.; Li, X. F.; Wang, J.; Emrick, T.; Long, S.; Wang, Q.; Balazs, A. C.; Russell, T. P. *Nature (London)* **2005**, *434*, 55–59.

(8) Thurn-Albrecht, T.; Schotter, J.; Kastle, G. A.; Emley, N.; Shibauchi, T.; Krusin-Elbaum, L.; Guarini, K.; Black, C. T.; Tuominen, M. T.; Russell, T. P. *Science* **2000**, *290*, 2126–2129.

(9) Boal, A. K.; Iihan, F.; DeRouchey, J. E.; Thurn-Albrecht, T.; Russell, T. P.; Rotello, V. M. *Nature (London)* **2000**, *404*, 746–748.

(10) (a) Yeh, S. W.; Wei, K. H.; Sun, Y. S.; Jeng, U. S.; Liang, K. S. *Macromolecules* **2003**, *36*, 7903–7907. (b) Yeh, S. W.; Wei, K. H.; Sun, Y. S.; Jeng, U. S.; Liang, K. S. *Macromolecules* **2005**, *38*, 6559–6566.

(11) Kim, B. J.; Chiu, J. J.; Yi, G. R.; Pine, D. J.; Kramer, E. J. *Adv. Mater.* **2005**, *17*, 2618–2622.

(12) (a) Lo, C. T.; Lee, B.; Winans, R. E.; Thiyagarajan, P. *Macromolecules* **2007**, *40*, 641–647. (b) Lee, B.; Lo, C. T.; Seifert, S.; Rago Dietz, N. L.; Winans, R. E.; Thiyagarajan, P. *Macromolecules* **2007**, *40*, 4235–4243.

(13) (a) Sohn, B. H.; Choi, J. M.; Yoo, S. I.; Yun, S. H.; Zin, W. C.; Jung, J. C.; Kanehara, M.; Hirata, T.; Teranishi, T. *J. Am. Chem. Soc.* **2003**, *125*, 6368–6369. (b) Bockstaller, M. R.; Lapetnikov, Y.; Margel, S.; Thomas, E. L. *J. Am. Chem. Soc.* **2003**, *125*, 5276–5277.

(14) Brust, M.; Walker, M.; Bethell, D.; Schiffrin, D. J.; Whyman, R. *J. Chem. Soc., Chem. Commun.* **1994**, 801–802.

(15) (a) Tenneti, K. K.; Chen, X.; Li, C. Y.; Tu, Y.; Wan, X.; Zhou, Q. F.; Sics, I.; Hsiao, B. S. *J. Am. Chem. Soc.* **2005**, *127*, 15481–15490. (b) Chen, H. L.; Lu, J. S.; Yu, C. H.; Yeh, C. H.; Jeng, U. S.; Chen, W. C. *Macromolecules* **2007**, *40*, 3271–3276.

(16) Rietveld, H. M. *J. Appl. Crystallogr.* **1969**, *2*, 65–71.

MA801364Y